

Evidence for Exponential Band Tails in Amorphous Silicon Hydride

T. Tiedje, J. M. Cebulka, D. L. Morel, and B. Abeles

Corporate Research Laboratories, Exxon Research and Engineering Co., Linden, New Jersey 07036

(Received 22 December 1980)

The width of the conduction- and valence-band tails in amorphous silicon hydride are inferred from time-of-flight measurements of the temperature dependence of the electron and hole drift mobilities, and a multiple-trapping model of dispersive transport.

PACS numbers: 72.20.Fr, 72.80.Ng

One of the fundamental distinguishing features of amorphous semiconductors is the presence of mobility edges in the density of states near the conduction- and valence-band edges.¹ In this Letter we report measurements of the shape of the localized state distribution near the conduction- and valence-band edges in thin films of glow-discharge amorphous silicon hydride (α -SiH_x). The properties of the band-tail states are inferred from time-of-flight (TOF) measurements of the temperature dependence of the electron and hole drift mobilities and the temperature dependence of the dispersion in the mobility, both interpreted in terms of a multiple-trapping model of dispersive transport.

A number of workers have studied the carrier drift mobilities in α -SiH_x in the past.²⁻⁴ However, the first measurements were made before the present understanding of dispersive transport had been developed,⁵ and as a result, the necessity to make the measurements at constant field and the significance of the temperature dependence of the dispersion parameter α were not recognized. These issues have not been resolved by more recent work.^{3,4} Consequently, the considerable amount of additional information about the distribution of localized states near the mobility edge, available in principle from the temperature dependence of the carrier transport process, has not been available in practice. In this Letter we report the first measurements of the temperature dependence of the dispersion in the electron and hole drift mobilities and explain the observed transition in the electron transport from dispersive to nondispersive near room temperature, in terms of a multiple-trapping model of dispersive transport.

The electron-drift-mobility measurements were made on a 3.9- μ m-thick film prepared by rf glow-discharge decomposition of silane as reported earlier.⁴ The measurements were performed on 2-mm² Schottky-diode structures consisting of (70 Å Pd)/(3.9 μ m α -SiH_x)/(500 Å n^+ -type α -SiH_x)/(100 Å Cr on a glass substrate).

Hole-drift-mobility measurements were also made on this film by exciting carriers through the Cr back contact; however the transit time could be identified only over a limited temperature range presumably because of deep hole traps. Although limited, the data on the hole drift mobility and its temperature dependence were similar to the results presented below for the boron-doped sample. The hole-drift-mobility measurements were made on a 1.7- μ m-thick dc glow-discharge film,⁴ doped with 1.7 ppm boron, as determined by secondary-ion mass spectroscopy analysis. Palladium Schottky-diode structures were also used for the hole transport measurements. In this case, the carriers were generated at the back contact which consisted of SnO₂ on glass without the n^+ -type α -SiH_x layer used in the electron sample. Electron transport could also be observed in this sample when carriers were generated at the Pd contact; however, the transit times were difficult to define and the electron collection efficiency was field dependent, once again presumably because of deep traps.

In the TOF experiment the photocurrent was excited with an 8-ns pulsed dye laser,⁴ with the sample in an evacuated hot stage or variable-temperature cryostat depending on the measurement temperature. The fast electron transients above room temperature were recorded directly on a Tektronix-7834 storage oscilloscope, while the rest of the data was recorded by a Biomation transient digitizer, with the oscilloscope used as a preamplifier. The data were recorded single shot, with the laser operating at a 1 Hz repetition rate, and at a low enough intensity that the density of photogenerated charge was at least an order of magnitude below the space-charge limit. Under these conditions no fatigue effects were observed in the photocurrent transients.

The electron photocurrent decay, following the light flash, is plotted on a log-log scale in the insets in Fig. 1 for two different temperatures. At low temperatures the photocurrent transients exhibit the power-law decays characteristic of dis-

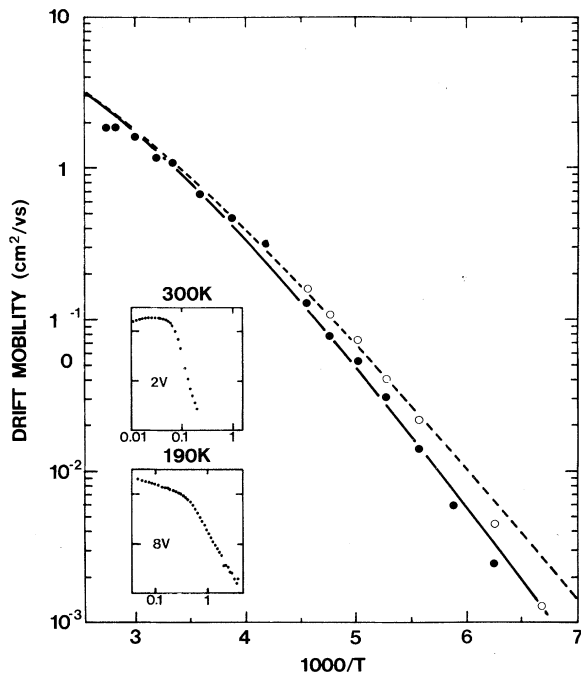


FIG. 1. Temperature dependence of the electron drift mobility for an electric field of 10^4 V/cm (closed circles) and 2×10^4 V/cm (open circles). The solid (broken) line is a fit to the low- (high-) field data with $T_c = 312$ K, $\mu_0 = 13$ cm²/V s and $\nu = 4.6 \times 10^{11}$ s⁻¹. The insets are representative photocurrent decays at 300 and 190 K plotted as $\log I$ vs $\log t$; the time scale is microseconds.

persive transport⁵ (see lower inset in Fig. 1) and at high temperatures the current decay has the abrupt falloff at the transit time characteristic of conventional diffusion-broadened transport (upper inset in Fig. 1). Thus the electron transport undergoes a transition from dispersive at low temperatures to nondispersive at high temperatures.

Also plotted in Fig. 1 is the electron drift mobility, defined by the standard expression $\mu_d = L^2 / Vt_T$, where L is the sample thickness and V is the applied bias. The transit time t_T was determined experimentally from the intersection point of linear fits to the two branches of the current decay on a log-log plot. The change in slope at the transit time becomes smaller at low temperatures, and hence t_T is more difficult to define. Thus the signal-to-noise ratio determines the low-temperature limit to the drift mobility measurements. The high-temperature limit is set by the temperature at which the dielectric relaxation time becomes comparable with the transit time.

The temperature dependence of the hole drift

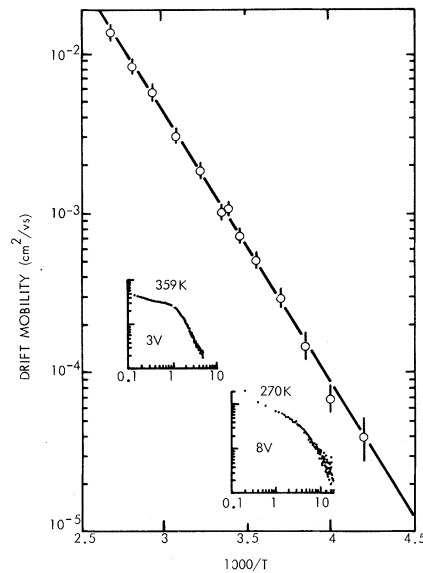


FIG. 2. Temperature dependence of the hole drift mobility for an electric field of 5.8×10^4 V/cm. The solid line is a fit to the data based on Eq. (1) with $T_c = 500$ K, $\mu_0 = 0.67$ cm²/V s and $\nu = 1.6 \times 10^{12}$ s⁻¹. The insets are representative photocurrent decays at 359 and 270 K plotted as $\log I$ vs $\log t$; the time scale is microseconds.

mobility measured on the boron-doped film is shown in Fig. 2. Like the electrons, the holes show more dispersion at low temperatures than at high temperatures; however, the hole transport is dispersive over the entire temperature range. The dispersion is normally characterized by a parameter α ($0 < \alpha < 1$ in the dispersive regime) which describes the slope of the current decay on a log-log scale, prior to the transit time (with exponent $\alpha - 1$) and after the transit time (with exponent $-\alpha - 1$). In Fig. 3, we plot the experimentally determined values of α , as a function of temperature for electrons and holes.

The simplest way to interpret these transport results is to use a multiple-trapping model⁵ in which one assumes that there is a mobility edge which is sharp compared to the width of the localized-state distribution, separating band states with finite mobility from gap states with zero mobility. We also assume that the localized states below the mobility edge are distributed exponentially in energy, all with equal capture cross sections. The release rates for carriers from these states are thermally activated and described by $\tau^{-1} = \nu \exp(-\epsilon/kT)$, where ϵ is the depth of the localized state below the mobility edge and ν is an

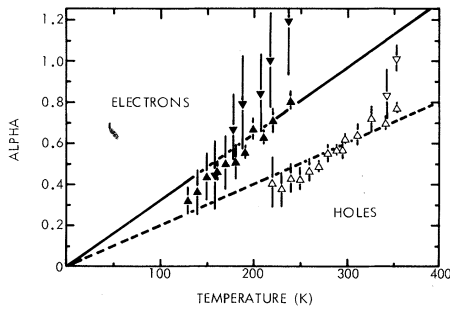


FIG. 3. Temperature dependence of the dispersion parameter α determined from the electron photocurrent decay before (closed triangles) and after (inverted closed triangles) the transit time, and for the holes before (open triangles) and after (inverted open triangles) the transit time. The lines are least-squares fits (of the form $\alpha = T/T_c$) to the data points, weighted by their relative accuracies. For electrons at high temperatures, $\alpha > 1$ corresponds to a current decay that is faster than t^{-2} , after t_T .

attempt rate.

With these assumptions, the photocurrent will have power-law decays of the form $t^{\alpha-1}$ before the transit time and $t^{-\alpha-1}$ after the transit time where the dispersion parameter $\alpha = T/T_c$.⁵ Here, kT_c is an energy which characterizes the width of the exponential band tail. The transit time, defined as the break point on the $\log I$ - $\log t$ plot is given by⁶

$$t_T \approx \nu^{-1} \left(\frac{\nu}{1-\alpha} \right)^{1/\alpha} \left(\frac{L^2}{\mu_0 V} \right)^{1/\alpha}, \quad (1)$$

for $T < T_c$. In this expression μ_0 is the "free carrier" mobility for an electron (or hole) in the band states just above the mobility edge.

The energy of photoinjected electrons is determined by a competition between thermalization which tends to push the electrons down in energy into the deepest localized states, and a density-of-states factor which favors high energies. For $T < T_c$, thermalization wins out and photoinjected electrons sink progressively deeper with increasing time and the transport is dispersive, while for $T > T_c$ the electrons remain concentrated near the mobility edge and the charge transport is non-dispersive, with drift mobility $\mu_0(1 - T_c/T)$.⁶ Thus we expect a transition from dispersive to nondispersive transport with increasing temperature, as is observed experimentally for electrons. A similar transition observed in *a*-Se may have the same origin.⁵ In the intermediate temperature regime close to T_c , where the transport

changes from dispersive to diffusive, the transit time can be calculated numerically from the expression for the time-dependent drift mobility,

$$\mu_D(t) \approx \mu_0 \frac{\alpha(1-\alpha)}{(\nu t)^{1-\alpha} - \alpha^2}, \quad (2)$$

derived as discussed earlier.⁶

The characteristic temperature of the conduction-band tail can be estimated from the temperature at which the electron transport becomes nondispersive or from the temperature dependence of the dispersion parameter shown in Fig. 3. Based on the fits to the data indicated by the lines in Fig. 3, the characteristic temperatures for the conduction- and valence-band tails are 312 and 500 K, respectively. Using these values for the widths of the band tails and the experimental values for L and V , we can determine μ_0 and ν by fitting the temperature dependence of the drift mobility by using Eqs. (1) and (2). The best fits are illustrated by the solid lines in Figs. 1 and 2. Note in Fig. 1 that the temperature dependence of the drift mobility exhibits a gradual change in slope near T_c as it changes from an exponential to a power-law dependence on T . This change in slope becomes progressively more abrupt as the sample thickness increases since the thermal activation energy for $T < T_c$ increases logarithmically with L [see Eq. (1)]. Also for $T < T_c$, the drift mobility is field dependent, according to Eq. (1). The good agreement between the measured and calculated field dependence shown in Fig. 1 provides an independent self-consistency check of the temperature-dependent α inferred from Fig. 3.

The material parameters indicated in the captions to Figs. 1 and 2, that were derived from the fits to the experimental drift-mobility data, are reasonable. For example, an electron free-carrier mobility of $13 \text{ cm}^2/\text{V s}$ corresponds to a mean free path of about four nearest-neighbor distances for an electron with thermal velocity 10^7 cm/s and a reduced effective mass of unity. Mean free paths of this order are generally expected for amorphous materials.¹ The smaller hole free-carrier mobility of $0.67 \text{ cm}^2/\text{V s}$ may reflect a larger effective mass or strong hole-lattice interactions.⁷ The attempt rates for release from traps can be related to capture cross sections by detailed balance.⁸ The experimental attempt rate of order 10^{12} s^{-1} for the conduction- and valence-band tail states implies a capture cross section of 10^{-15} cm^2 , if we assume a band-edge degeneracy of 10^{20} cm^{-3} . This capture

cross section is of atomic dimensions, as expected for neutral centers.

Even though there is no well-defined cutoff energy in the distribution of band-tail states in our model, to a good approximation the drift mobility has the exponential temperature dependence characteristic of a single trap level. Rather than reflecting a cutoff in the density of states below the band edge,⁹ the activation energy arises from a kinetic limit to how deep a photoexcited carrier is able to sink into the band tail before being collected. We see no evidence of a change in activation energy at low temperatures that would indicate a transition to hopping transport, as reported by LeComber and Spear.² Whether the absence of a transition to hopping in our data is caused by a different distribution of gap states or by a difference in the interpretation of the TOF data remains to be resolved.

In summary, the excellent agreement between the model and the experimental data lends considerable support to multiple trapping as the mechanism of charge transport in α -SiH_x. The experimental results are consistent with electron and hole free-carrier mobilities of 11 and 0.67 cm²/Vs, respectively, and with exponential valence- and conduction-band tails 500 and 312 K wide, respectively.¹⁰ The transition near room temperature in the electron transport from dispersive to nondispersive is interpreted as the temperature at which kT equals the characteristic width

of the conduction-band tail.

We thank G. D. Cody and C. R. Wronski for valuable discussions and A. Rose for suggestions that inspired the interpretation in this paper.

¹N. F. Mott and E. A. Davis, *Electronic Processes in Non-Crystalline Materials* (Oxford Univ. Press, New York, 1979), 2nd ed.

²P. G. LeComber and W. E. Spear, *Phys. Rev. Lett.* **25**, 509 (1970).

³A. R. Moore, *Appl. Phys. Lett.* **31**, 762 (1977); D. Allan, *Philos. Mag. B* **38**, (1978); J. Mort, *S. Grammatica*, J. C. Knights, and R. Lujan, *Solar Cells* **2**, 451 (1980).

⁴T. Tiedje, B. Abeles, D. L. Morel, T. D. Moustakas, and C. R. Wronski, *Appl. Phys. Lett.* **36**, 695 (1980); T. Tiedje, C. R. Wronski, B. Abeles, and J. M. Cebulka, *Solar Cells* **2**, 301 (1980).

⁵G. Pfister and H. Scher, *Adv. Phys.* **27**, 747 (1978).

⁶T. Tiedje and A. Rose, *Solid State Commun.* **37**, 49 (1981).

⁷C. Tsang and R. A. Street, *Phys. Rev. B* **19**, 3027 (1979).

⁸A. Rose, *Concepts in Photoconductivity and Allied Problems* (R. E. Krieger Publishing Co., Huntington, N.Y., 1978).

⁹W. E. Spear, D. Allan, P. LeComber, and A. Ghaith, *Philos. Mag. B* **41**, 419 (1980).

¹⁰Although sensitive to different energy levels in the gap, by extrapolation, recent deep-level transient spectroscopy data [J. D. Cohen, D. V. Lang, and J. P. Harbison, *Phys. Rev. Lett.* **45**, 197 (1980)] is consistent with the band-tail widths inferred here.

Scaling Laws in CsNiF₃ with Applied Magnetic Field: An Optical Study

J. Cibert and Y. Merle d'Aubigné

*Laboratoire de Spectrométrie Physique, Université Scientifique et Médicale de Grenoble,
F-38041 Grenoble, France*

(Received 19 February 1981)

Results on spin dynamics in CsNiF₃ with applied magnetic fields are obtained through a detailed study of the shape of a sharp near-infrared absorption line. In a rather extended field and temperature range, a universal curve connects the linewidth to the temperature when $(JH)^{1/2}$ is used as an energy unit. The relevance of the reduced variable $k_B T / (JH)^{1/2}$ to the existence of solitons is discussed.

PACS numbers: 75.40.-s, 75.30.Ds, 78.40.Ha

A great deal of theoretical work has been directed recently towards the study of solitons in condensed matter physics. From an experimental point of view one-dimensional (1D) magnetic systems seem to be rather promising, and both a ferromagnet (CsNiF₃) and an antiferromagnet

[tetramethylammonium manganese chloride (TMMC)] have revealed quasielastic neutron scattering about which solitons have been invoked. CsNiF₃ had been extensively studied some years ago as a good physical realization of a 1D S=1 easy-plane ferromagnet. A fairly complete de-